

Excited-State Dynamics of Cytosine Tautomers

Kyriaki Kosma, Christian Schröter, Elena Samoylova, Ingolf Volker Hertel, and Thomas Schultz*

Max Born Institute, Max-Born-Strasse 2A, D-12489, Berlin-Adlershof, Germany

Received August 31, 2009; E-mail: schultz@mbi-berlin.de

Abstract: We report the relaxation dynamics of keto and enol or keto–imino cytosine, photoexcited in the wavelength range of 260–290 nm. Three transients with femtosecond to hundreds of picoseconds lifetimes are observed for the biologically relevant keto tautomer and are assigned to internal conversion and excited-state tautomerization. Only two transients with femtosecond and picosecond lifetimes are identified for the enol or keto–imino tautomer and are assigned to internal conversion processes. The results are discussed in the context of published ab initio theory.

Introduction

The characterization of photochemical and photophysical processes in isolated DNA bases (adenine, thymine, cytosine, and guanine) may help to understand the photostability of DNA upon UV irradiation. One crucial mechanism discussed in this context is rapid excited-state relaxation, which ensures that the molecules relax back to their ground state before excited-state reactions can occur.¹

All DNA bases have multiple tautomers with sometimes differing photochemical properties. In this context, cytosine is of particular interest because three tautomers have been identified in molecular beam microwave spectroscopy with an estimated abundance of 1:1:0.25 for keto:enol:keto–imino.² Experimental results for isolated molecules in molecular beams can be directly compared to theoretical predictions, and cytosine can therefore serve to explore the photochemical properties of biologically relevant tautomers. In this work, we distinguish the keto and enol or keto–imino tautomers of cytosine by exciting the molecules with five different wavelengths in the range of 260–290 nm. We present the first femtosecond time-resolved data for the biologically relevant keto cytosine and propose an excited-state tautomerization reaction to the keto–imino tautomer. We also show that existing literature data are dominated by contributions from the enol or keto–imino tautomer.

In Figure 1 we show the three relevant cytosine tautomers. According to theoretical predictions, the enol form is the most stable tautomer in the gas phase.^{3–5} The keto form is predicted to be 33 meV less stable in the gas phase,⁵ but is the biologically relevant tautomer found in nucleotides where the ring N–H hydrogen is substituted with a ribose sugar moiety. Crystalline cytosine exists only in the keto form as shown by X-ray

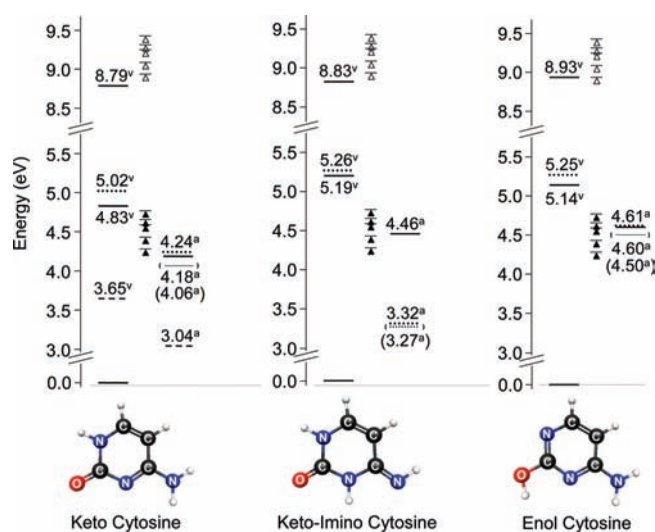


Figure 1. Structures and state energies for the keto, keto–imino, and enol tautomers of cytosine. Relative energies for the ground states and vertical (v) and adiabatic (a) excitation energies for the bright $1\pi\pi^*$ (solid lines) and dark $1n\pi^*$ states (dotted lines) are taken from DFT/MRCI calculations of Tomić et al.⁵ Values in brackets include zero-point energy corrections and are in good agreement with experimental data. State energies for a $3\pi\pi^*$ state in keto cytosine (dashed lines) stem from a CASPT2 calculation by Merchán et al.¹⁵ Vertical ionization potentials are given as calculated by Dolgounitcheva et al.¹² We photoexcited cytosine with five different wavelengths in the range 260–290 nm (photon energy marked by ▲) and ionized in a three-photon process with 800 nm (total photon energy marked by ▼).

diffraction studies.⁶ The existence of other tautomers in gas-phase experimental studies was explained by tautomerization in cytosine clusters via concerted proton transfer during thermal evaporation.⁷ The keto–imino tautomer is predicted to be the least stable of the three tautomers with a ground-state energy 55 meV above that of the enol.⁵

Keto and enol tautomers of cytosine were observed and identified in UV–IR double-resonance multiphoton ionization

(1) Crespo-Hernandez, C. E.; Cohen, B.; Hare, P. M.; Kohler, B. *Chem. Rev.* **2004**, *104*, 1977–2019.

(2) Brown, R. D.; Godfrey, P. D.; McNaughton, D.; Pierlot, A. P. *J. Am. Chem. Soc.* **1989**, *111*, 2308–2310.

(3) Kobayashi, R. *J. Phys. Chem. A* **1998**, *102*, 10813–10817.

(4) Trygubenko, S. A.; Bogdan, T. V.; Rueda, M.; Orozco, M.; Luque, F. J.; Spöner, J.; Slavicek, P.; Hobza, P. *Phys. Chem. Chem. Phys.* **2002**, *4*, 4192–4203.

(5) Tomić, K.; Tatchell, J.; Marian, C. M. *J. Phys. Chem. A* **2005**, *109*, 8410–8418.

(6) Barker, D. L.; Marsh, R. E. *Acta Crystallogr.* **1964**, *17*, 1581.

(7) Yang, Z. B.; Rodgers, M. T. *Phys. Chem. Chem. Phys.* **2004**, *6*, 2749–2757.

(REMPI) experiments:^{8–10} A spectrum with a band origin at 31 826 cm⁻¹ (3.95 eV, 314 nm) was assigned to the keto tautomer, and a spectrum with a band origin close to 36 000 cm⁻¹ (4.46 eV, 278 nm) was assigned to the enol tautomer. Nanosecond time-resolved data with excitation close to the band origin of keto cytosine revealed a transient with 290 ns lifetime. An intersystem crossing to a triplet state was inferred to explain this long lifetime.⁸

Tomić et al.⁵ used density functional theory/multireference configuration interaction (DFT/MRCI) calculations to predict the energies of optically bright ¹ππ* and optically dark ¹nπ* singlet excited states for all three tautomers. The ¹ππ* adiabatic excitation energies of 4.06 eV (305 nm) for the keto and 4.50 eV (276 nm) for the enol tautomer are in very good agreement with the REMPI experimental values. In the keto–imino tautomer, the calculated adiabatic excitation energy for the bright ¹ππ* (4.46 eV, 278 nm) is far above that of a dark ¹nπ* state (3.32 eV). Ionization potentials for keto cytosine¹¹ or all tautomers¹² were calculated to be below 9 eV, in agreement with experimental data where available. We summarize the calculated energy levels for the relevant excited and ionic states in Figure 1.

Femtosecond pump–probe experiments in the gas phase measured the excited-state lifetimes of cytosine with an excitation wavelength of 267^{14,15} and 250 nm.¹⁶ The excited-state decays were modeled with a Gaussian function and a monoexponential decay with 3.2 ps lifetime,¹⁴ a biexponential decay with 160 fs and 1.86 ps lifetimes,¹⁵ and a biexponential decay with below 100 fs and 1.2 ps lifetimes.¹⁶ Internal conversion processes between ¹ππ*, ¹nπ*, and the ground state were discussed to explain the fast excited-state relaxation. None of the time-resolved studies discussed the tautomers responsible for the fast excited-state relaxation, but according to the REMPI results and theory, all three tautomers may be observed with 267 or 250 nm excitation.

Ab initio calculations focused mostly on the description of excited states and conical intersections in the keto tautomer and proposed decay channels that proceed via the ¹ππ*, ¹n_Oπ* (electron excitation from the oxygen lone pair), and ¹n_Nπ* (electron excitation from the ring nitrogen lone pair) singlet excited states. To facilitate the interpretation of our own pump–probe experiments, we discuss the calculations with a particular focus on the expected photophysical behavior.

First complete active space self-consistent field (CASSCF) calculations^{17,18} predicted a readily accessible conical intersection between the ¹ππ* and ¹n_Oπ* states, the latter being lower

in energy. CASSCF results are very sensitive to the active space and level of theory, and more elaborate studies using CASSCF and CASPT2 methods found that both the ¹n_Nπ* and the ¹ππ* states are energetically below the ¹n_Oπ* state.¹⁹ According to the CASPT2 results, the ¹ππ* and ¹n_Nπ* states are near-degenerate, and the conical intersections for ¹ππ*–¹nπ* internal conversion are accessible through energetic barriers of 250 meV or more for the ¹n_Oπ* and 120 meV or more for the ¹n_Nπ* state. A direct “ethylenic” relaxation path from the ¹ππ* state to the ground state can be reached through a lower barrier of approximately 100 meV.^{19–22} Multiple parallel relaxation pathways involving the ¹ππ* and both ¹nπ* states were found using the CAS multiple spawning technique,²³ and the results reproduced features of the time-resolved electron spectrum after 250 nm excitation.¹⁶

Ab initio MRCI²⁴ and DFT MRCI⁵ calculations predicted a similar or identical ethylenic relaxation path to lead almost barrierless from the ¹ππ* state to the ground state. The energy of the ¹n_Oπ* state and ¹n_Nπ* state is predicted to be higher than the lowest ¹ππ* state; hence a population of the ¹nπ* states is not expected. Coupled cluster calculations identified a biradical state, which intersects with the ¹ππ* and ground state and could offer an alternative internal conversion pathway.^{25,26} To summarize these theoretical results, we may expect ultrafast relaxation of the photochemically excited ¹ππ* state to the ground state via one or more conical intersections. The population of ¹nπ* states seems plausible, but does not seem to represent the lowest energy pathway for excited-state relaxation.

Merchán et al.¹³ predicted some probability for populating the lowest triplet state ³ππ* in the keto tautomer due to a near degeneracy of singlet and triplet states near the ¹ππ* potential energy minimum. This is in line with similar predictions for the other pyrimidine bases thymine and uracil.^{27,28}

Only DFT/MRCI calculations are available for the enol and keto–imino tautomers⁵ and identified the lowest excited states with ¹ππ* and ¹n_Nπ* character as shown in Figure 1. For the enol tautomer, the authors identified no conical intersections with the ground state and proposed that low-lying vibrational levels in the ¹ππ* state decay by “normal” internal conversion, possibly through coupling to nearby ¹n_Nπ* levels. For the keto–imino tautomer, easily accessible conical intersections between the first excited ¹ππ* state, a lower-lying ¹n_Nπ* state, and the electronic ground state were predicted. The ¹n_Nπ* minimum is more than 0.7 eV below the lowest identified conical intersection from S₁ to the ground state, and we expect correspondingly long lifetimes for this state.

- (8) Nir, E.; Müller, M.; Grace, L. I.; de Vries, M. S. *Chem. Phys. Lett.* **2002**, *355*, 59–64.
 (9) Nir, E.; Plützer, C.; Kleinermanns, K.; de Vries, M. *Eur. Phys. J. D* **2002**, *20*, 317–329.
 (10) Nir, E.; Hünig, I.; Kleinermanns, K.; de Vries, M. S. *Phys. Chem. Chem. Phys.* **2003**, *5*, 4780–4785.
 (11) Roca-Sanjuan, D.; Rubio, M.; Merchán, M.; Serrano-Andres, L. *J. Chem. Phys.* **2006**, *125*, 10768–10779.
 (12) Dolgounitcheva, O.; Zakrzewski, V. G.; Ortiz, J. V. *J. Phys. Chem. A* **2003**, *107*, 822–828.
 (13) Merchán, M.; Serrano-Andres, L.; Robb, M. A.; Blancafort, L. *J. Am. Chem. Soc.* **2005**, *127*, 1820–1825.
 (14) Kang, H.; Lee, K. T.; Jung, B.; Ko, Y. J.; Kim, S. K. *J. Am. Chem. Soc.* **2002**, *124*, 12958–12959.
 (15) Canuel, C.; Mons, M.; Piuze, F.; Tardivel, B.; Dimicoli, I.; Elhanine, M. *J. Chem. Phys.* **2005**, *122*, 074316.
 (16) Ullrich, S.; Schultz, T.; Zgierski, M. Z.; Stolow, A. *Phys. Chem. Chem. Phys.* **2004**, *6*, 2796–2801.
 (17) Ismail, N.; Blancafort, L.; Olivucci, M.; Kohler, B.; Robb, M. A. *J. Am. Chem. Soc.* **2002**, *124*, 6818–6819.
 (18) Blancafort, L.; Robb, M. A. *J. Phys. Chem. A* **2004**, *108*, 10609–10614.

- (19) Blancafort, L. *Photochem. Photobiol.* **2007**, *83*, 603–610.
 (20) Merchán, M.; Serrano-Andres, L. *J. Am. Chem. Soc.* **2003**, *125*, 8108–8109.
 (21) Sobolewski, A. L.; Domcke, W. *Phys. Chem. Chem. Phys.* **2004**, *6*, 2763–2771.
 (22) Merchán, M.; Gonzalez-Luque, R.; Climent, T.; Serrano-Andres, L.; Rodriguez, E.; Reguero, M.; Pelaez, D. *J. Phys. Chem. B* **2006**, *110*, 26471–26476.
 (23) Hudock, H. R.; Martinez, T. J. *ChemPhysChem* **2008**, *9*, 2486–2490.
 (24) Kistler, K. A.; Matsika, S. *J. Phys. Chem. A* **2007**, *111*, 2650–2661.
 (25) Zgierski, M. Z.; Fujiwara, T.; Kofron, W. G.; Lim, E. C. *Phys. Chem. Chem. Phys.* **2007**, *9*, 3206–3209.
 (26) Zgierski, M. Z.; Fujiwara, T.; Lim, E. C. *Chem. Phys. Lett.* **2008**, *463*, 289–299.
 (27) Serrano-Perez, J. J.; Gonzalez-Luque, R.; Merchán, M.; Serrano-Andres, L. *J. Phys. Chem. B* **2007**, *111*, 11880–11883.
 (28) Etinski, M.; Fleig, T.; Marian, C. *J. Phys. Chem. A*, ASAP article, DOI: 10.1021.

The $^1n_N\pi^*$ state in the keto–imino tautomer of cytosine is by far the lowest excited singlet state of all tautomers, and we should consider excited-state tautomerization from the keto or enol tautomer into this state. The keto to keto–imino tautomerization resembles an ultrafast amine to imine excited-state tautomerization discussed for 2-aminopyridine based on photoelectron spectra²⁹ and ab initio theory.³⁰ Because of a possible near degeneracy of $^1\pi\pi^*$ and $^1n_N\pi^*$ states in the keto tautomer¹⁹ and enol tautomer,⁵ the reaction barriers for excited-state tautomerization may be low.

We can conclude that the excited states in the biologically relevant keto tautomer have been thoroughly investigated by theory, whereas those in the enol and keto–imino tautomer have drawn much less interest. Yet to this date, no time-resolved data with subnanosecond resolution can be unambiguously assigned to the isolated keto tautomer. Comparison of theory with experimental data is therefore problematic. In this work, we distinguish the keto, enol, and keto–imino tautomers by exciting the molecules with five different wavelengths in the range of 260–290 nm. We present the first femtosecond time-resolved data for the biologically relevant keto cytosine and show that literature data are dominated by contributions from the enol or keto–imino tautomers.

Experimental Section

Cytosine (Sigma-Aldrich, 97% purity) was evaporated in a metal oven at temperatures around 240 °C. Using helium as a carrier gas (1–1.5 bar), the sample was expanded through a heated pulsed valve (modified General Valve, Series 9) with a repetition rate of 70 Hz, limited by the gas load in the source chamber. The resulting cold molecular beam passed through a 1 mm skimmer to reach the ionization region. Ions were detected in a Wiley–McLaren time-of-flight mass spectrometer along the molecular beam axis. A multichannel-plate detector was placed off axis to the molecular beam to avoid deposition of neutral molecules. The ion trajectories were steered by deflector plates behind the ion acceleration region. A commercial kHz titanium sapphire (Ti:Sa) fs-oscillator/amplifier system delivered 2 mJ, 800 nm, sub-50 fs pulses. Tuning of the pump wavelength occurred via an optical parametric amplifier, followed by frequency up-conversion in nonlinear crystals. Cytosine was photoexcited (pumped) with 260, 267, 270, 280, and 290 nm pulses. Pulses of 800 nm were used to ionize (probe) the photoexcited molecules. To suppress higher-order absorption processes, the energies of the pump (1–2 μ J) and probe beams (500 μ J) were attenuated until the ionization rate was approximately 1 ion per laser shot. A 1+3' (UV+IR') photon process with 290 nm excitation is sufficient for ionizing keto cytosine (total photon energy of 8.93 eV), and a 1+3' photon process with excitation at 280–260 nm is sufficient for the ionization of both the keto and the enol tautomers (total photon energy >9.09 eV, see Figure 1). A mechanical delay stage was used to delay the probe pulses for time-resolved measurements. A computer-controlled data acquisition routine collected mass spectra at different pump–probe delays. For each mass spectrum, the signals for $(2–2.5) \times 10^3$ laser shots were averaged. The yield of cytosine ions was recorded as a function of the pump–probe delay for time ranges up to 200 ps. Negative times correspond to the probe pulses arriving first. The mass spectra of cytosine showed the parent mass (111 u) and several fragment ions, the most dominant being masses 66, 67, 68, and 69 u and masses 40, 41, and 42 u. The fragments are the same as those observed in

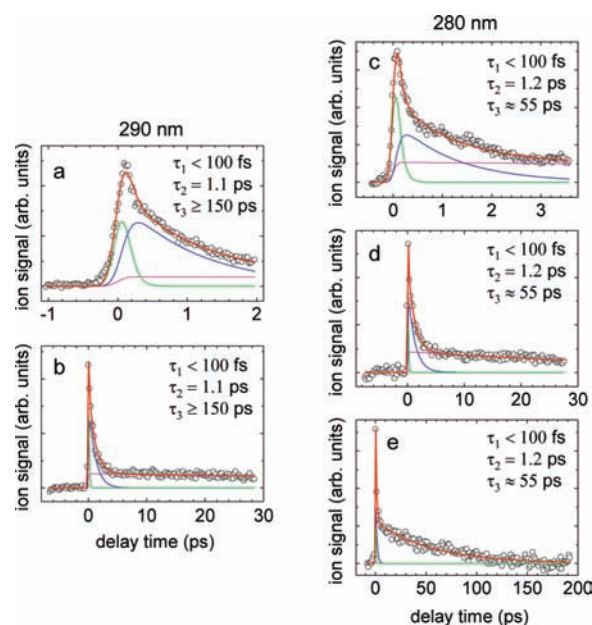


Figure 2. Time-dependent total ion signals for cytosine excited with 290 nm (a,b) and 280 nm (c–e) and ionized with 800 nm. The experimental data (○) are shown together with the full fit (red line) and the individual exponential components (colored lines).

electron-impact ionization mass spectra.³¹ The parent and fragment transients exhibited identical transient lifetimes (indicative of fragmentation in the ionic state, see ref 32) and were added together. This helped to improve the signal-to-noise ratio and resulted in a constant baseline at negative and positive delays: fragmentation resulted in bleaching of the parent ion signals at positive delay times, but the corresponding ion signal was merely transplanted into fragment ion channels. The data were subsequently fitted by a sum of exponential decays, convoluted with the cross-correlation function between the pump and the probe pulses (temporal width of about 150 fs). Up to three exponential components with lifetimes τ_1 , τ_2 , and τ_3 were found to contribute to the signals. Lifetimes below 100 fs are not fully resolved and are given as $\tau < 100$ fs. The transients reflect the decaying population in the excited states that participate in the relaxation process after initial photoexcitation.

Results

Figure 2a,b shows the time-resolved ion yield of cytosine excited at 290 nm (4.28 eV) together with multiexponential fit curves. The excitation energy is below the origin of the bright states in the enol or keto–imino tautomer (see Figure 1), and we assign the observed transients to the keto tautomer. Three exponential components with lifetimes of $\tau_1 < 100$ fs, $\tau_2 = 1.1$ ps, and $\tau_3 \geq 150$ ps are necessary to reproduce the observed signals.

Figure 2c–e displays the time-resolved ion yield of cytosine excited at 280 nm (4.43 eV), close to, but still below, the reported enol and keto–imino absorption bands. Again, three exponential decays are necessary to reproduce the recorded signals. The shorter lifetimes of $\tau_1 < 100$ fs and $\tau_2 = 1.2$ ps are comparable to those observed with 290 nm excitation. The lifetime of the long-lived transient $\tau_3 \approx 55$ ps is shorter as compared to the 290 nm data.

(29) Samoylova, E.; Radloff, W.; Ritze, H. H.; Schultz, T. J. *Phys. Chem. A* **2009**, *113*, 8195–8201.

(30) Zhang, F.; Ai, Y. J.; Luo, Y.; Fang, W. H. *J. Chem. Phys.* **2009**, *130*, 144315.

(31) Linstrom, P.; Mallard, W., Eds. *NIST Chemistry WebBook, NIST Standard Reference Database Number 69*; National Institute of Standards and Technology: Gaithersburg, MD; <http://webbook.nist.gov>, (retrieved October 27, 2009).

(32) Samoylova, E.; Smith, V. R.; Ritze, H. H.; Radloff, W.; Kabelac, M.; Schultz, T. J. *Am. Chem. Soc.* **2006**, *128*, 15652–15656.

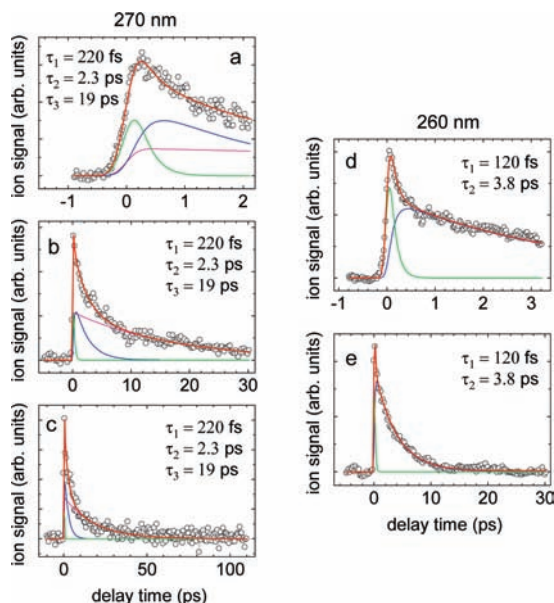


Figure 3. Time-dependent total ion signals of cytosine excited with 270 nm (a–c) and 260 nm (d,e) and ionized with 800 nm. The experimental data (○) are shown together with the full fit (red curve) and the individual exponential components (colored lines).

With excitation at 270 nm (4.59 eV) and 260 nm (4.77 eV), we can expect to observe also the enol and keto–imino tautomers. Three exponential decays are necessary to reproduce the traces for 270 nm excitation as shown in Figure 3a–c. The longer scans exhibit a longer-lived transient with $\tau_3 = 19$ ps, originating probably from the corresponding long-lived state observed for the keto tautomer. The shorter lifetimes $\tau_2 = 2.3$ ps and $\tau_1 = 220$ fs are significantly different from the values found for the keto tautomer. The lifetime τ_2 is between the respective values observed for the keto tautomer at 280 and 290 nm (approximately 1.2 ps) and for the observed transients at 260 nm excitation (3.8 ps, see below). Unfortunately, exponential fits are not capable to distinguish the sum of exponential contributions with moderately different lifetimes from a single exponential with an intermediate lifetime, and we can only suggest that the transient with lifetime τ_2 is the sum of contributions from several tautomers.

Figure 3d,e shows the results for 260 nm excitation where the observed lifetimes $\tau_1 = 120$ fs and $\tau_2 = 3.8$ ps are longer than the corresponding lifetimes upon 280 and 290 nm excitation. A contribution from a third, long-lived component is not obvious at this excitation wavelength. We propose that the different lifetimes τ_1 and τ_2 are due to the enol or keto–imino tautomer.

For comparison with the literature,^{14,15} we present a transient for cytosine excited at 267 nm, measured up to 7 ps delay time in Figure 4. The data can be reproduced with only two exponential decays. To account for a possible long-lived species, we allowed for a “background signal” at positive delays (pink line) during the fitting process, and we obtain a somewhat better fit with lifetimes $\tau_1 = 210$ fs and $\tau_2 = 2.2$ ps, in good agreement with our results at 270 nm and the values reported in the literature,¹⁵ $\tau_1 = 160$ fs and $\tau_2 = 1.86$ ps.

Discussion

Table 1 summarizes the excited-state lifetimes for all transients observed at excitation wavelengths in the range of 260–290 nm. REMPI spectra^{8,9} identified the origin of the UV

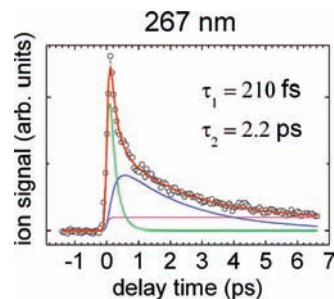


Figure 4. Time-dependent ion signals with a pump wavelength of 267 nm and a probe wavelength of 800 nm. The experimental values (○) are shown together with the full fit (red line) and the individual exponential components (colored lines).

Table 1. Excited-State Lifetimes for All Transients at Excitation Wavelengths $\lambda = 260$ – 290 nm

λ (nm)	τ_1 (ps)	τ_2 (ps)	τ_3 (ps)
260	0.12	3.8	
267	0.21	2.2	long
270	0.22	2.3	19
280	<0.1	1.2	55
290	<0.1	1.1	≥ 150

absorption bands of gas-phase keto and enol cytosine at a respective wavelength of 314 and 278 nm. Ab initio calculations are in good agreement with these values and predict the origin of the keto–imino tautomer at 278 nm⁵ (see Figure 1 for all relevant vertical and adiabatic energy levels). We can therefore assign the dynamics observed at 280 and 290 nm to the keto tautomer. The data measured above the enol and keto–imino band origin (260, 267, and 270 nm) may stem from all three tautomers, but the keto–imino tautomer is predicted to be less stable^{3–5} and may play a minor role.

The data recorded for 290 nm show three transients with lifetimes of $\tau_1 < 100$ fs, $\tau_2 = 1.1$ ps, and a much slower decay with $\tau_3 \geq 150$ ps. Results at 280 nm are qualitatively similar with τ_3 being shorter. We can therefore postulate a relaxation of the photoexcited bright $^1\pi\pi^*$ state via two intermediate (dark) states. Recent theoretical investigations of the keto tautomer, however, proposed a direct decay channel from the photoexcited $^1\pi\pi^*$ state to the ground state via easily accessible conical intersections (see Introduction).^{5,19,20,22,24,26} We therefore propose that the ultrafast component with lifetime τ_1 is due to vibrational dynamics in the $^1\pi\pi^*$ state and the motion of the wavepacket away from the Franck–Condon region. Internal conversion from the $^1\pi\pi^*$ to the ground state can explain the second transient with lifetime τ_2 . The picosecond lifetime for $^1\pi\pi^*$ to ground-state internal conversion is in agreement with a moderate barrier of approximately 100 meV predicted by CASSCF/CASPT2 calculations,^{19,20,22} but not with a barrierless process. Another plausible explanation might assume the population of $^1n\pi^*$ states despite the theoretically predicted barriers for $^1\pi\pi^*$ to $^1n\pi^*$ internal conversion.

To explain the third transient with lifetime τ_3 , we must postulate the involvement of an additional dark state. This state may be the same as that observed by Nir et al.,⁸ who measured a 290 ns lifetime at the keto cytosine band origin and proposed that the observed transient is due to a triplet state. Merchán et al.¹³ also predicted the possibility of populating the lowest triplet state $^3\pi\pi^*$ due to a near degeneracy of $^1\pi\pi^*$ singlet and $^3n\pi^*$ triplet states near the $^1\pi\pi^*$ potential energy minimum. The long-lived transient observed here may therefore originate from

intersystem crossing to the triplet state manifold. The large amplitude of the long-lived transient in our data upon 290, 280, and 270 nm excitation indicates a considerable quantum yield for this relaxation channel. Population flow into the triplet must compete with the direct $^1\pi\pi^*$ to ground-state relaxation within the measured τ_2 lifetime of 1.1–1.2 ps; hence the singlet–triplet coupling must be astonishingly large.

Merchán et al.¹³ suggest that the carbonyl group present in keto cytosine might be a key structural element facilitating fast intersystem crossing. Our experimental observation of a long-lived transient in keto cytosine would support this hypothesis. Further support for this hypothesis might be drawn from a recent report of very fast (sub-10 ps) intersystem crossing in solvated thymine³³ (a pyrimidine base with two carbonyl groups) and corresponding theoretical predictions for the isolated molecule.^{27,28}

Despite the theoretical predictions, we are skeptical whether the singlet–triplet coupling can be large enough to explain efficient intersystem crossing on the time scale of 1 ps. We therefore offer an alternative explanation for the third transient based on excited-state tautomerization into the low energy $^1n_N\pi^*$ state of the keto–imino tautomer (cf., Figure 1). According to CASSCF and CASPT2 calculations,¹⁹ the adiabatic energy of the corresponding $^1n_N\pi^*$ state is near-degenerate with that of the lowest $^1\pi\pi^*$ state in the keto tautomer. In the keto–imino tautomer, DFT/MRCI calculations show that this $^1n_N\pi^*$ state is more than 1 eV below the $^1\pi\pi^*$ state. We can therefore expect strong stabilization of the $^1n_N\pi^*$ state along the tautomerization coordinate, and this might suppress reaction barriers for the amine to ring-nitrogen hydrogen transfer. The energy of the $^1n_N\pi^*$ state is more than 0.7 eV below the lowest identified conical intersection with the ground state.⁵ This $^1n\pi^*$ state may therefore act as a population trap and explain the observed long lifetime τ_3 . A high barrier for $^1n\pi^*$ state relaxation in the keto–imino tautomer would also agree with the strong wavelength dependence observed for lifetime τ_3 .

With excitation at 267 nm, the two observed lifetimes $\tau_1 = 210$ fs and $\tau_2 = 2.2$ ps reproduce approximately the lifetimes of 160 fs and 1.86 ps reported in the literature.¹⁵ However, our experimental data do not fully decay to zero within the limited pump–probe delay range and are best simulated assuming a longer-lived pedestal toward positive pump–probe delays. The data with 270 nm excitation show very similar results, exhibiting a well-resolved longer-lived transient with a lifetime of $\tau_3 = 19$ ps. We assign this long-lived transient to the corresponding state in the keto tautomer and assume that we excite a mixture of keto and enol or keto–imino tautomers at these wavelengths. Different tautomer distributions might explain why the existing literature reported different excited-state lifetimes in the short wavelength region despite very similar experimental procedures.^{14,15}

Only two transients are identified in the time-resolved spectra upon 260 nm excitation: An ultrafast decay with $\tau_1 = 120$ fs is followed by a slower relaxation step with $\tau_2 = 3.8$ ps, but the long-lived component is absent or very weak. A similar lifetime of 3.5 ps is described in the literature¹⁴ upon excitation with 267 nm. The longer lifetimes τ_1 and τ_2 observed at this shorter wavelength are assigned to a dominant contribution from the enol, or possibly the keto–imino tautomer.

For the keto–imino tautomer, Tomić et al.⁵ predicted conical intersections between the bright $^1\pi\pi^*$ state and the $^1n\pi^*$ and ground state. The $^1n\pi^*$ minimum is well below the bright $^1\pi\pi^*$

state and more than 0.7 eV below a conical intersection to the ground state. The short lifetime τ_1 described here would agree with fast internal conversion of the bright $^1\pi\pi^*$ state to the $^1n\pi^*$ and ground states through conical intersections. Yet the second transient with lifetime τ_2 is too short-lived to agree with a 0.7 eV barrier for internal conversion of the $^1n\pi^*$ state, and we therefore propose that the observed transients are dominated by contributions from the enol tautomer.

No conical intersection between S_1 and the ground state was predicted for the enol tautomer. Instead, Tomić et al. suggested that low-lying vibrational levels in the $^1\pi\pi^*$ state decay through coupling to nearby $^1n\pi^*$ levels. The experimentally determined short lifetimes τ_1 and τ_2 would indicate a strong coupling between $^1\pi\pi^*$ and $^1n\pi^*$ states and raise the question whether yet-unidentified conical intersections between those states and the ground state might exist. Despite the much lower energy of the $^1n\pi^*$ state in the keto–imino tautomer, we observe no indications for enol to keto–imino tautomerization in the excited state. In a theoretical study of the DNA base thymine,³⁴ tautomerization barriers for a corresponding hydrogen transfer from oxygen to ring-nitrogen were found to be large, and we propose that excited-state tautomerization plays no role in enol cytosine.

Conclusion

We have given a first report on the ultrafast excited-state dynamics of the biologically relevant keto tautomer of cytosine. Observed transients with femtosecond and picosecond lifetimes agree with the theoretical prediction of fast, but not barrierless excited-state relaxation via conical intersections between the $^1\pi\pi^*$ and ground state.⁵ A third transient is due to the population of an excited state with a lifetime of a few tens of picoseconds (at 270 nm) to hundreds of picoseconds (at 290 nm). We propose that this state is a low-lying $^1n\pi^*$ state in the keto–imino tautomer, populated by excited-state tautomerization. In the condensed phase, we may expect rapid back hydrogen-transfer catalyzed by hydrogen-bound water molecules;^{35–37} hence this relaxation pathway would agree with the expected high photostability of DNA constituents. We should mention that the population of a $^3\pi\pi^*$ triplet state was predicted by theory¹³ and could offer an alternative explanation for the observed data. Yet the population of a long-lived triplet state should dramatically reduce the photochemical stability of cytosine and would therefore run contrary to expectations.

The excited-state relaxation dynamics of the keto tautomer described here are markedly different from the ultrafast relaxation reported for the wavelength range 266–250 nm.^{14–16} On the basis of our data, we assign the latter to dominant contributions from the enol, or possibly the keto–imino tautomer at wavelengths below 270 nm.

Acknowledgment. We thank Frank Noack for his support by providing the laser system in the femtosecond application laboratory of the Max-Born-Institut Berlin. We thank Wolfgang Radloff, Werner Fuss, Lluís Blancafort, and Hans-Hermann Ritze for fruitful discussions and helpful comments. Financial support by the Deutsche Forschungsgemeinschaft through SFB-450 is gratefully acknowledged.

JA907355A

(34) Gonzalez-Vazquez, J.; Gonzalez, L.; Samoylova, E.; Schultz, T. *Phys. Chem. Chem. Phys.* **2009**, *11*, 3927–3934.

(35) Podolyan, Y.; Gorb, L.; Leszczynski, J. *Int. J. Mol. Sci.* **2003**, *4*, 410–421.

(36) Mazzuea, D.; Marino, T.; Russo, N.; Toscano, M. *THEOCHEM* **2007**, *811*, 161–167.

(37) Fogarasi, G. *Chem. Phys.* **2008**, *349*, 204–209.

(33) Hare, P. M.; Crespo-Hernandez, C. E.; Kohler, B. *Proc. Natl. Acad. Sci. U.S.A.* **2007**, *104*, 435–440.